Effectiveness Factors for Porous Catalysts

J. O. MINGLE and J. M. SMITH

Northwestern University, Evanston, Illinois

From the equations expressing mass and energy transfer in the solid and void regions of a catalyst of micropores, conversion and temperature profiles are evaluated as a function of the properties of the particle and the reaction system. The method developed is illustrated with numerical calculations for a first-order, irreversible reaction. Microeffectiveness factors E_c are derived from these profiles for several distribution functions for the size (radius) of the micropores.

The results indicate that the nature of the pore-size distribution cannot affect E_c more than about 10%. However effectiveness factors greater than unity are possible for exothermic reactions with high heats of reaction and particles of reasonable size.

To treat pelletted catalysts, equations are also developed for determining conversion and temperature profiles in pellets formed by compressing the microporous particles These results are interpreted in terms of macroeffectiveness factors E_s, with values of E_c applicable at various positions in the pellet. To illustrate the method of solution numerical values of E_s are determined for a limited range of parameters. The results indicate that in pelletted catalysts large temperature gradients may exist. For an exothermic reaction this can lead to a significant increase in macroeffectiveness factor.

The total rate of a chemical reaction on a porous catalyst pellet depends upon the extent of the internal surface and the size of the pores comprising this surface. The effectiveness of the internal surface is influenced by the temperature and the composition of the reacting mixture within the pellet. Diffusional resistance within the pores reduces the concentration in the direction toward the center of the pellet and thus lowers the rate of reaction. For an exothermic reaction the thermal resistance leads to a higher temperature within the pellet, and this increases the rate of reaction on the internal surface. The purpose of this investigation is to determine the effects of concentration and temperature gradients on the effectiveness of the internal surface for reaction, taking into account the distribution of pore sizes in the catalyst pellet. The procedure for doing this will be to evaluate the conversion and temperature profiles within the pellet and then sum up the local reaction rates corresponding to each element of internal surface. Two cases are considered. In the first the catalyst consists of an assembly of micropores only, such as in silica gel. In the second pelletted materials are studied which are formed by compressing small particles containing the micropores. In the resulting pellets there is a distribution of macropores between the particles as well as a distribution of micropores within the particles. After a brief summary of the previous work in this area, a model of a catalyst pellet is proposed as a basis for calculation of the concentration and temperature profiles.

PREVIOUS STUDIES

Many porous catalysts have most of their pores with radii smaller than 200Å. Under commonly encountered conditions of temperature and pressure this size pore is considerably smaller than the mean free path of the gas, so that Knudsen (*10*) diffusion occurs. Since the Knudsen diffusivity is given by

$$D_k = \frac{2}{3} r \left(\frac{8 R_g T}{\pi M} \right)^{1/2} \qquad (1)$$

the diffusion flux is pressure independent but dependent upon the pore size and temperature. Wheeler (*15*) has empirically generalized this result to cover the transition range from Knudsen to bulk diffusion. His diffusion coefficient is

$$D = \frac{1}{2} \epsilon D_B (1 - e^{-D_k/D_B}) \qquad (2)$$

In a pioneer study Thiele (*14*) considered the effect of diffusion, but not heat transfer, on reaction rates in porous catalysts. In other words the catalyst particle was assumed to be at a uniform temperature throughout. The following expression was obtained for the effectiveness factor:

$$E^T = \frac{1}{h} \tanh h \qquad (3)$$

where

$$h^2 = 2 L^2 k / r_e D_e \qquad (4)$$

Wheeler evaluated the effective diffusivity in accordance with Equation (2) and the effective pore radius as

$$r_e = \frac{2V_g}{S_g} = \bar{r} \qquad (5)$$

Equation (3) is for slab geometry, but other geometries have been investigated by Aris (*1*) and found to give similar results.

More recently, temperature effects have been considered by Schulson (*11*), who evolved a numerical solution procedure for a Thiele type of model, and Beek (*2*), who used a linearized model also to study multiple reactions.

Henry (*5*) has measured diffusion rates in an alumina catalyst pellet and obtained an effective radius for Knudsen diffusion about 10% larger than that predicted by Equation (5). Bokhoven and van Raayen (*3*), in studies with an ammonia catalyst, found large differences between observed values of r_e and those given by Equation (5); however bulk diffusion may have been significant in their work.

CATALYST MODEL

In this study, a porous catalyst pellet is defined to mean the material formed by compressing a large number of small porous particles. This compression introduces a macroscopic pore-size distribution between the particles whose pores are within the range 200 to 10,000 Å. (*6*) so that bulk diffusion

should predominate. The normal microscopic pore distribution still exists within the catalyst granules and is normally within the Knudsen diffusion-size range. The distribution of micropore sizes can be analytically approximated by the method proposed by Mingle (9). This concept of a pellet fits such materials as pelletted alumina particles which show both a macro and micropore-size distribution. A homogeneous material such as silica gel contains no macropores. For a substance like this only the part of the following development concerned with micropore effectiveness factors need be considered.

The small microporous particles will be assumed to conform to the following model:

1. The various sizes and lengths of pores can be represented by straight cylindrical pores of constant length with a radius governed by a pore-size distribution, $Z(r)$.
2. All of the pore radii are within the range where Knudsen diffusion predominates.
3. Because of the interconnections between the actual pores the effective radius for Knudsen diffusion is αr, where α is assumed a constant independent of r. The numerical value of α can be obtained from measurement or prediction of diffusion rates (5).
4. An irreversible, surface chemical reaction of order n occurs on the walls of the pores with a rate constant governed by an Arrhenius (11) type of expression.
5. The heat of reaction is constant and is transferred to the pore mouth by conduction through only the solid phase of the catalyst. The equations are written in terms of effective thermal conductivity k_s/ϵ based upon the void area of the pore.
6. Concentration and temperature gradients exist only along the length of the pore; that is no radial gradients exist.
7. The average reaction rate for the particle can be obtained by averaging the individual pore reaction rates over the pore-size distribution.

The assumptions governing the macroassembly of particles (the macropore region) consist of the following:

1. The macroregion is homogeneous.
2. The reaction at any point is the reaction rate for the conditions prevalent at that point times the microeffectiveness factor evaluated for those same point conditions.
3. Mass transfer effects are determined by bulk diffusion.
4. Heat transfer through the pellet is by conduction with a thermal conductivity of k_s', based upon the total area.
5. The conditions at the surface of the pellet are constant.

By means of the above model, temperature and concentration gradients are computed and used to evaluate effectiveness factors.

MICROEFFECTIVENESS FACTORS

The differential equations expressing the concentration and temperature within a single pore of radius are

$$\frac{d}{dz}\left(D_{Ke}\frac{dC}{dz}\right) - \frac{2}{r}k_n C^n = 0 \quad (6)$$

$$\frac{d^2T}{dz^2} + \frac{2Q\epsilon k_n C^n}{r k_s} = 0 \quad (7)$$

These equations can be put in dimensionless form by defining the following variables:

$$\theta = (T - T_o)/T_o \quad (8)$$

$$X = (C_o - C)/C_o \quad (9)$$

$$\xi = z/L \quad (10)$$

$$k_n = A_n e^{-E/R_g T} = k_{no} e^{B_o\theta/(1+\theta)} \quad (11)$$

$$D_{ke} = \frac{2r_e}{3}\left(\frac{8R_g T}{\pi M'}\right)^{1/2}$$

$$= \overline{D}_{k_o}\left(\frac{\alpha r}{r_e}\right)(1+\theta)^{1/2} \quad (12)$$

$$\Psi_1 = \frac{2L^2 \bar{r} k_{no} C_o^{n-1}}{\alpha r^2 \overline{D}_{k_o}} \quad (13)$$

$$\Psi_2 = \frac{2Q L^2 \epsilon k_{no} C_o^n}{r k_s T_o} \quad (14)$$

In terms of these quantities Equations (6) and (7) become

$$\frac{d^2X}{d\xi^2} + \frac{1}{2(1+\theta)}\frac{d\theta}{d\xi}\frac{dX}{d\xi} + \frac{\Psi_1(1-X)^n}{(1+\theta)^{1/2}} e^{B_o\theta/(1+\theta)} = 0 \quad (15)$$

$$\frac{d^2\theta}{d\xi^2} + \Psi_2(1-X)^n e^{B_o\theta/(1+\theta)} = 0 \quad (16)$$

The Linear Case

Under certain instances Equations (15) and (16) can be reduced to a form that is analytically solvable. The assumptions necessary for this are that the diffusion coefficient and the reaction rate are constant (independent of temperature), and that the chemical reaction is first order, irreversible.

This set of assumptions constitute what is called the *linear case*. It is noted that these assumptions do not preclude a temperature gradient in the particle but do require that the conversion gradient and ultimately the effectiveness factor not be affected by the temperature variation. In this paper analytical solutions are presented first for the linear case; then numerical solutions are given for the more general, or nonlinear, case defined by Equations (15) and (16).

For this linear case the microdifferential equations reduce to the form

$$\frac{d^2X}{d\xi^2} + \Psi_1(1-X) = 0 \quad (17)$$

$$\frac{d^2\theta}{d\xi^2} + \Psi_2(1-X) = 0 \quad (18)$$

The boundary conditions are chosen so as to isolate the pore; that is

$$X'(1) = \theta'(1) = \theta(0) = X(0) \quad (19)$$

The solution of Equations (17) through (19) for the conversion X and dimensionless temperature is

$$X_l = 1 - \cosh(\Psi_1^{1/2}\xi) + \tanh(\Psi_1^{1/2})\sinh(\Psi_1^{1/2}\xi) \quad (20)$$

$$\theta_l = \frac{\Psi_2}{\Psi_1}X \quad (21)$$

From these expressions the derivatives at the pore mouth are evaluated as

$$X_l'(0) = \Psi_1^{1/2}\tanh(\Psi_1^{1/2}) \quad (22)$$

$$\theta_l'(0) = \Psi_3\tanh(\Psi_1^{1/2}) \quad (23)$$

where

$$\Psi_3 = \frac{\Psi_2}{\Psi_1^{1/2}} \quad (24)$$

Evaluation of Effectiveness Factors

To determine the effectiveness factor for the particle of micropores the reaction rate for a single pore of radius r is first evaluated. This latter quantity may be expressed in terms of the concentration gradient at the pore mouth or the rate of reaction on the pore surface. Equation (25) denotes the equality of these two expressions:

$$-\pi r^2 D_{K_{eo}}\frac{dC(0)}{dz} = \int_o^L 2\pi r k_n C^n dz = 2\pi r L\,\overline{k_n C^n} \quad (25)$$

The bar indicates an average value for one pore. If now the rate per pore is averaged over the distribution of micropores in the particle, there is obtained

$$\int_o^\infty 2\pi r L\,\overline{k_n C^n}\,Z(r)\,dr = \overline{\overline{k_n C^n}}\int_o^\infty 2\pi r L Z(r)\,dr \quad (26)$$

where the double bar indicates an average value for the catalyst particle. The microeffectiveness factor is defined as the actual reaction rate compared with the rate if all the internal surface were available at pore mouth conditions. In terms of Equations (25) and (26) E_e is given by

$$E_c = \frac{\overline{k_n C^n}}{k_{n_o} C_o^n}$$

$$= \frac{\int_o^\infty r k_n C^n Z(r)\,dr}{k_n C_o^n \int_o^\infty r Z(r)\,dr}$$

$$= \frac{-\int_o^\infty D_{K_{eo}} C'(0) r^2 Z(r)\,dr}{2k_{n_o} C_o^n \int_o^\infty r Z(r)\,dr} \quad (27)$$

Expressed in terms of the dimensionless parameter Ψ_1 this is

$$E_c = \frac{\int_o^\infty \Psi_1^{-3} X'(0) Z(\Psi_1)\,d\Psi_1}{\int_o^\infty \Psi_1^{-2} Z(\Psi_1)\,d\Psi_1} \quad (28)$$

where $Z(\Psi_1)$ is the pore-size distribution in terms of Ψ_1. In this paper two types of distribution functions will be used, a pseudo-Maxwellian and a Gaussian. Written in terms of Ψ_1 these are

$$Z^M(\Psi_1) = A^M \Psi_1^{-1/2}\, e^{-a_j(\overline{\Psi}_1/\Psi_1)^{1/2}} \quad (29)$$

$$Z^G(\Psi_1) = A^G\, e^{-\beta^2[a_j(\overline{\Psi}_1/\Psi_1)^{1/2}-1]^2} \quad (30)$$

The value of a is 3, 1.1246, and 1.0200 for a Maxwellian, Gaussian ($\beta = 2$) and Gaussian ($\beta = 5$) pore-size distribution function, respectively.

Equations (27) or (28) are general expressions for E_c within the limitation of the stated assumptions. Either of these along with the solutions to Equations (15) and (16) constitute the solution to the general case. While the results must be obtained by numerical methods, they can be expressed in equation form by adding a deviation term to the analytical solution for the linear case. Equations (31) through (35) illustrate the results for a particle with pores of a single size.

In this limiting situation of uniform pore size the distribution function is

$$Z^{G-\infty} = A^G\, \delta(\Psi_1 - \overline{\Psi}_1) \quad (31)$$

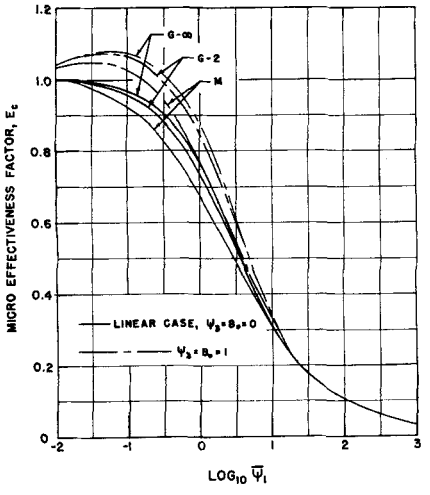

Fig. 1. Pore-size distribution effect on microeffectiveness factor.

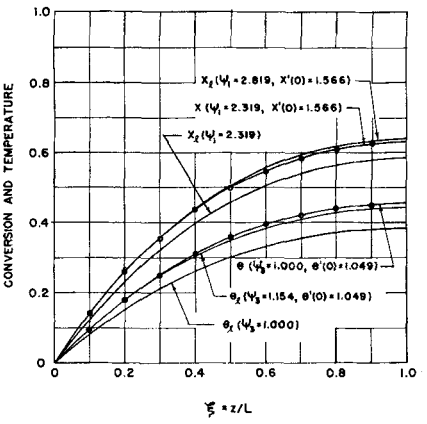

Fig. 2. Micropore conversion and temperature profiles, $\psi_1 = 2.319$, $\psi_3 = 1$, $B_o = 1$.

which corresponds to a β value of infinity. One obtains the effectiveness factor from Equation (28), using Equation (31):

$$E_c^{G-\infty} = \frac{X'(0, \overline{\Psi}_1)}{\overline{\Psi}_1} \quad (32)$$

The derivative of the conversion profile at the pore mouth can be represented as the sum of the linear-case contribution, from Equation (22), and a deviation term as follows:

$$X'(0) = X_l'(0) + \Delta X'(0)$$

$$= \Psi_1^{1/2} \tanh \Psi_1^{1/2} + \Delta X'(0) \quad (33)$$

Substituting this expression in Equation (32) one gets

$$E_c^{G-\infty} = \overline{\Psi}_1^{-1/2} \tanh(\overline{\Psi}_1^{1/2}) + \frac{\Delta X'(0)}{\overline{\Psi}_1}$$

$$= E_c^T + \frac{\Delta X'(0)}{\overline{\Psi}_1} \quad (34)$$

The last equality comes from the fact that for the linear case for one pore size

$$\overline{\Psi}_1 = h^2 \quad (35)$$

Comparing Equation (35) and Equation (3) one sees that the first term in Equation (34) is simply the Thiele effectiveness factor. It will be referred to as the *Thiele number*. With this approach the quantity $\Delta X'(0)/\overline{\Psi}_1$ represents the deviation of E_c due to nonlinear effects. Equations (31), (32), and (34) are restricted to the limiting size distribution $G - \infty$. The general solution is represented by Equations (15), (16), and (28).

EVALUATION OF MICROEFFECTIVENESS FACTORS

The effect of pore-size distribution on the microeffectiveness factor for the linear case is shown by some of the curves in Figure 1. The pore-size distributions cover the practical range encountered physically, since the Maxwellian function represents a wider than normal spread. The Gaussian ($\beta = 5$) and Gaussian ($\beta = \infty$) are identical within the accuracy shown in Figure 1. The effect of size distribution is seen to be small, with a maximum of 10% deviation for a small range near $\overline{\Psi}_1$ values of unity.

The nonlinear differential Equations (15) and (16) were solved, with an IBM-650 digital computer, for a range of values of Ψ_3, B_o, Ψ_1 and for Maxwellian and Gaussian pore distributions. The specific combinations of numerical values of these variables for which solutions were obtained are shown in Table 1*. Only a first-order, irreversible reaction was considered. Temperature and conversion profiles are illustrated in Figure 2 for specific values of the parameters. Also included on the figure are linear-case profiles with adjusted parameters identified as X_l ($\Psi_1 = 2.819$) for the conversion profile and θ_l ($\Psi_3 = 1.154$) for the temperature. The close agreement between the two cases suggests that a variation of parameter technique (6) might be employed as an alternate means of solution.

Figure 3 illustrates the variation of the initial derivative of the conversion profile with the micro-mass-transfer parameter, Ψ_1. A curve for the linear case is also included on the plot. The complete results are shown in Table 2.* Effectiveness factors were evaluated from Equation (28) for various pore-size distributions with the data in Table 2. The results are presented in Table 3 and illustrated for two cases by the dotted curves in Figure 1. It is noted that effectiveness factors greater than unity are obtained for Thiele numbers near 0.1. The highest value calculated was over 12 (Table 3). However these

* Tabular material has been deposited as document 6622 with the American Documentation Institute, Photoduplication Service, Library of Congress, Washington 25, D. C., and may be obtained for $1.25 for photoprints or for 35-mm. microfilm.

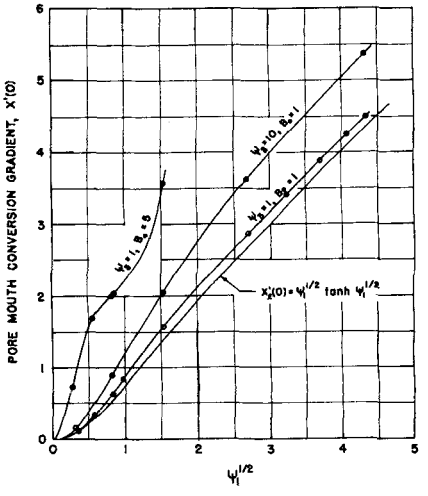

Fig. 3. Mass and heat transfer effects on pore mouth conversion gradient.

TABLE 3. EFFECTIVENESS FACTORS FOR MICROPOROUS PARTICLES BASED UPON EQUATION (28)

Ψ_3	B_o	$\text{Log}_{10}\overline{\psi_1}$	E_c^M	E_c^{G-2}	$E_c^{G-\infty}$
1	1	−1	1.029	1.064	1.069
		0	0.765	0.844	0.884
		1	0.327	0.333	0.333
		2	0.100	0.100	0.100
10	1	−1	1.379	1.424	1.607
		0	1.023	1.136	1.192
		1	0.403	0.410	0.417
		2	0.103	0.100	0.100
1	5	−1	12.7	10.6	11.4
		0	2.59	2.45	2.38
		1	0.593	1.52	0.800
		2	0.107	0.283	0.100
0*	0*	−1	0.922	0.956	0.968
		0	0.675	0.733	0.762
		1	0.305	0.313	0.315
		2	0.100	0.100	0.100

* $\psi_3 = B_o = 0$ constitutes the linear case.

high results are misleading, since external mass transfer effects have been neglected, and since the heat of reaction necessary to obtain the required parameter values is usually high. An effectiveness factor greater than unity is possible for only an exothermic reaction, that is a positive value of Ψ_3.

The nonlinear contribution to E_c, defined by Equation (34) for particles with uniform pore size, is illustrated in Figure 4 for certain values of Ψ_3 and B_o. The curve for $\Psi_3 = 1$ is especially useful because the deviation from linear behavior is itself a straight-line function of the combined variable $\Psi_3 B_o$, provided this variable is less than or equal to unity. This condition results in

$$E_c(\Psi_3, B_o, \overline{\Psi_1}) = E_c^T(\overline{\Psi_1}) + \Psi_3 B_o \Delta E_c(\overline{\Psi_1}, \Psi_3 = 1, B_o = 1) \quad (36)$$

MACROEFFECTIVENESS FACTORS

If the catalyst consists of a pellet of microporous particles, the previous results for E_c can be used for the effectiveness factor of each particle. The value of E_c will change depending upon the location of the particle in the pellet because the temperature and conversion change. Hence it is necessary to evaluate the conversion and temperature profiles in the pellet with the local values of E_c before an over-all pellet effectiveness factor E_s can be determined. When one uses the prementioned assumptions for the macropore region, differential equations for conversion and temperature written in vector notation are

$$\nabla \cdot (D' \nabla C) - \rho S_g E_c k_n C^n = 0 \quad (37)$$

$$k_s' \nabla^2 T + \rho S_g Q E_c k_n C^n = 0 \quad (38)$$

These expressions can be made dimensionless by introducing the variables

$$X_s = \frac{C_s - C}{C_s} \quad (39)$$

$$\theta_s = \frac{T - T_s}{T_s} \quad (40)$$

$$\zeta = r/R \quad (41)$$

and defining the parameters

$$\varphi_1 = \rho S_g R^2 k_{ns} C_s^{n-1}/D' \quad (42)$$

$$\varphi_2 = \rho S_g R^2 Q k_{ns} C_s^n / k_s' T_s \quad (43)$$

$$B_s = \frac{E}{R_g T_s} \quad (44)$$

It may be noted that

$$k_n = k_{ns} e^{B_s \theta_s/(1+\theta_s)} \quad (45)$$

and

$$D' = D_s'(1+\theta_s)^{1/2}/(1 + f X_s) \quad (46)$$

When one uses these variables and

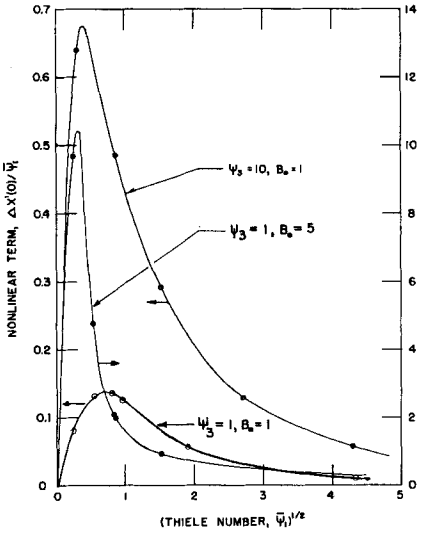

Fig. 4. Nonlinear contribution to microeffectiveness factor.

definitions, Equations (37) and (38) become

$$\frac{d^2X_s}{d\zeta^2} + \frac{1}{2(1+\theta_s)}\frac{d\theta_s}{d\zeta}\frac{dX_s}{d\zeta} - \frac{f}{1+fX_s}\left(\frac{dX_s}{d\zeta}\right)^2 + \frac{\lambda_s}{\zeta}\frac{dX_s}{d\zeta} + \frac{\varphi_1 E_c (1-X_s)^n (1+fX_s)}{(1+\theta_s)^{1/2}} e^{B_s\theta_s/(1+\theta_s)} = 0 \quad (47)$$

$$\frac{d^2\theta_s}{d\zeta^2} + \frac{\lambda_s}{\zeta}\frac{d\theta_s}{d\zeta} + \varphi_2 (1-X_s)^n E_c e^{B_s\theta_s/(1+\theta_s)} = 0 \quad (48)$$

The symbol λ_s equals 0, 1, or 2 for slab, cylindrical, or spherical geometry, respectively.

The microeffectiveness factor is a function of $\overline{\Psi_1}$, Ψ_3, and B_o, which in themselves are functions of X_s and θ_s. Relating these parameters to their values at the pellet surface, one gets the functional relationship of E_c as

$$E_c = E_c(\overline{\Psi_1}, \Psi_3, B_o) = E_c\{\overline{\Psi_{1s}} (1-X_s)^{n-1}(1+\theta_s)^{-1/2} e^{B_s\theta_s/(1+\theta_s)}, \Psi_{3s}(1-X_s)^{\frac{n+1}{2}}(1+\theta_s)^{3/4} e^{B_s\theta_s/2(1+\theta_s)}, B_s/(1+\theta_s)\} \quad (49)$$

In pellets the temperature gradients in the small microporous particles generally are small. Hence each microparameter can be evaluated separately, and it is only necessary to look up E_c as a function of $\overline{\Psi_1}$, as in Table 2.

The macroeffectiveness factor E_s is defined as the actual reaction rate compared with the surface reaction rate if both were utilizing the total internal surface area. An equation for E_s can be developed by writing the two expressions for the rate of the reaction, just as was done for the microcase in Equation (25). In terms of the average rate

$$E_s = \frac{\overline{E_c k_n C^n}}{k_{ns} C_s^n} = \frac{-D_s' \lambda_g \nabla C(R)}{\rho S_g R k_{ns} C_s^n} \quad (50)$$

Here λ_g/R is the ratio of surface to volume and is 3, 2, or 1 for a sphere, cylinder, or slab, respectively. In dimensionless form Equation (50) becomes

$$E_s = -\lambda_g \nabla X_s(1)/\varphi_1 \quad (51)$$

This is the final expression for E_s for the model proposed. The integrations of Equations (47) and (48), along with Equation (51), comprise the solution for the general case.

As in the microporous particle, Equations (47) and (48) can be solved analytically for the linear case. To do this it is noted that for spherical pellets Equation (47) and (48) reduce to

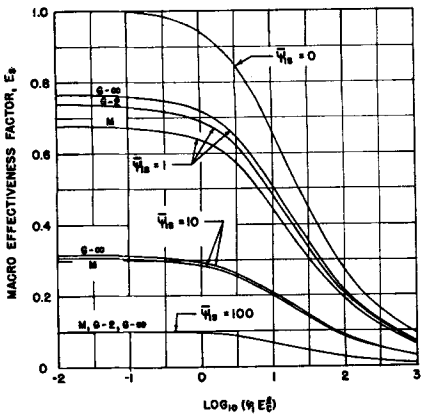

Fig. 5. Micropore distribution effects on macroeffectiveness factors, linear case.

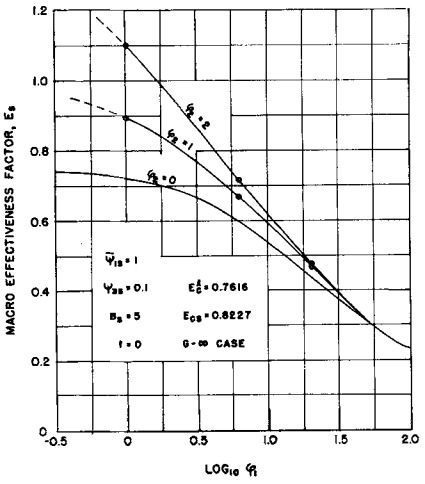

Fig. 6. Mass and heat transfer effects on macroeffectiveness factor.

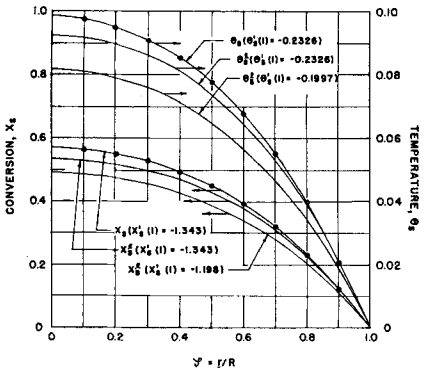

Fig. 7. Macroparticle conversion and temperature profiles, $\varphi_1 = 6$, $\varphi_2 = 1$, $\bar{\psi}_{1s} = 1$, $\psi_{3s} = 0.1$, $B_s = 5$, $f = 0$, $G - \infty$ case.

$$\frac{d^2 X_s}{d\zeta^2} + \frac{2}{\zeta}\frac{dX_s}{d\zeta} + \varphi_1 E_c(1 - X_s) = 0 \quad (52)$$

$$\frac{d^2 \theta_s}{d\zeta^2} + \frac{2}{\zeta}\frac{d\theta_s}{d\zeta} + \varphi_2 E_c(1 - X_s) = 0 \quad (53)$$

The boundary conditions are

$$X_s(1) = \theta_s(1) = X_s'(0) = \theta_s'(0) = 0 \quad (54)$$

Here E_c is a function only of $\bar{\Psi}_1$. This quantity is a constant for the linear case. Then the solution of Equations (52), (53), and (54) is

$$X_s = 1 - \frac{\sinh(\Lambda\zeta)}{\zeta \sinh\Lambda} \quad (55)$$

$$\theta_s = \varphi_2 X_s/\varphi_1 \quad (56)$$

where

$$\Lambda = (\varphi_1 E_c)^{1/2} \quad (57)$$

Substituting the conversion gradient obtained by differentiating Equation (55) in Equation (51) one gets the macroeffectiveness factor for the linear case. The result is

$$E_s = \frac{3}{\varphi_1}(\Lambda \coth\Lambda - 1) = \frac{3E_c}{\Lambda^2}(\Lambda\coth\Lambda - 1) \quad (58)$$

EVALUATION OF MACROEFFECTIVENESS FACTORS

The effect of micropore-size distribution on the effectiveness factor for the whole pellet can be obtained for the linear case from Equation (58), since only E_c is affected by this distribution. Figure 5 shows this effect to be a maximum near a value of $\bar{\Psi}_{1s}$ equal to unity and to decrease as $\bar{\Psi}_{1s}$ changes to lower or higher values. As in gel type of catalysts the deviation due to micropore-size distribution is less than 10% at all times, with the Gaussian ($\beta = \infty$) distribution giving the highest value and the Maxwellian the lowest value. Variations of the same order of magnitude would be expected to apply to nonlinear cases. Harriott (3) has proposed a treatment of the combined effect of micro and macroeffectiveness factors that is similar to Equation (58) except that no distribution of pore sizes is used.

In evaluating the nonlinear case only first order exothermic reactions were considered. Equations (47) and (48) were solved numerically on the computer and E_s values computed from Equation (51) for the parameter values shown in Table 1 and for a uniform ($G - \infty$) micropore-size distribution. The results are presented in

Table 5. Illustration of Calculation of Micro and Macro Effectiveness Factors for a Typical Catalyst

Quantity	Case 1	Case 2
n	1	1
ρ—g./cc.	1.3	1.3
S_g—sq. m./g.	310	310
R—cm.	0.2	0.2
k_{ns}—cm./sec.	7.43×10^{-6}	7.43×10^{-6}
C_s—g. moles/cc.	3×10^{-5}	3×10^{-5}
Q—cal./g. mole	2.32×10^{3}	8.88×10^{3}
k_s'—cal./(cm. sec. °K.)	8×10^{-4}	8×10^{-4}
T_s—°K.	400	400
D_s'—sq. cm./sec.	0.2	0.2
ϵ	0.5	0.5
L—cm.	0.01	0.01
$\bar{r}$—Å.	22	22
$\bar{D}_{ks}$—sq. cm./sec.	6.75×10^{-3}	6.75×10^{-3}
E—cal./g. mole	3,980	3,980
M'	40	40
α	1.0	1.0
k_s—cal./(cm. sec. °K.)	8×10^{-4}	8×10^{-4}
$\bar{\Psi}_{1s}$	1	1
ψ_{3s}	0.1	3.83×10^{-3}
B_s	5	5
φ_1	6	6
φ_2	260	1
f	0	0
$E_c{}^1$	0.762	0.762
E_{cs}	0.822	0.762
E_s	—	0.65

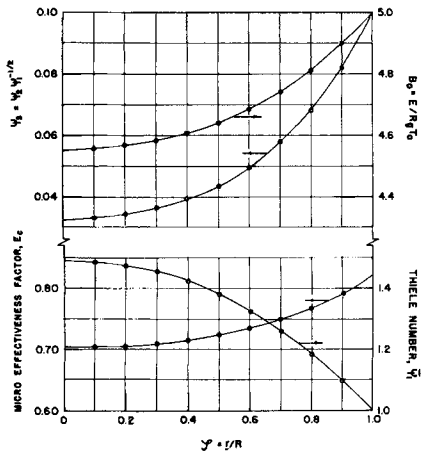

Fig. 8. Variation of microparameters E_c, B_o, ψ_3, $\bar{\psi}_1$ within macroparticle, $\varphi_1 = 6$, $\varphi_2 = 1$, $\bar{\psi}_{1s} = 1$, $\psi_{3s} = 0.1$, $B_3 = 5$, $f = 0$, $G - \infty$ case.

Table 4.* The individual parameters were chosen primarily to show the magnitude of nonlinear effects rather than be physically representative. To illustrate the relationship between the parameters and the properties of the reaction and catalyst, two specific cases are shown in Table 5. The effectiveness factors shown were taken from plots of the data of Table 4. Case 1 is calculated so as to produce a Ψ_{3s} value of 0.1 and has a very high heat of reaction, as well as a rather slow reaction rate constant. Case 2 is calculated to produce a φ_2 value of unity and shows a reasonable heat of reaction. Under these latter circumstances the Ψ_{3s} value becomes quite low and leads to a negligible nonlinear contribution to the effectiveness factor for the microregion. This is indicated in the table by the equivalence of $E_c{}'$ and the effectiveness factor E_{cs} evaluated at the conditions of the pellet surface. On the other hand the microeffectiveness factor for Case 1 increases over the linear solution value owing to the temperature variation through the pellet. A value of E_s is not shown for Case 1 because it is beyond the range of computations. It would be enormous as a result of the very large temperature gradient. In contrast E_s for Case 2 is less than E_c because the temperature gradient is negligible, allowing the diffusion resistance in the macropores to decrease the effectiveness factor of the pellet as a whole.

It is to be noted that temperature effects are greatly accentuated in the macropellet because of its larger size. The ratio of the corresponding parameters for the macro and microcases is

$$\varphi_1/\bar{\Psi}_{1s} = \rho\, S_g R^2 \alpha \bar{r}\, \bar{D}_{ks}/2\, L^2 D_s' \cong 10 \qquad (59)$$

$$\varphi_2/\Psi_{3s}\, \bar{\Psi}_{1s}{}^{1/2} = \rho\, S_g R^2 \bar{r} k_s/ \qquad 2L^2 \epsilon k_s' \cong 1000 \qquad (60)$$

The numbers are approximate values for a silica-alumina type of porous catalyst. For mass transfer the ratio of $(R/L)^2$ is compensated for by the D_{ks}/D_s' ratio. However this effect is missing in the heat transfer case, since $k_s/\epsilon k_s'$ does not vary from unity to a very large degree.

The effectiveness factors from Table 4 are shown graphically in Figure 6. The lines of constant φ_2 represent changes in the heat of reaction. Since Equation (55) shows no maximum with φ_1, the temperature will continue to rise as φ_1 is reduced; that is the bulk diffusion coefficient increases. Changing the reaction rate constant will effect both φ_1 and φ_2 so that this effect cannot be shown simply in Figure 6.

* See footnote on page 245.

The resulting conversion and temperature profiles are shown for a single set of values of φ_1 and φ_2 in Figure 7. In this case the adjusted linear profiles, identified as $X_s{}'[X_s'(1) = -1.343]$ for the conversion profile and as $\theta_s{}'[\theta_s'(1) = -0.2326]$ for the temperature profile, do not fit as well as for the microcase. The variation of the microparameters $\bar{\Psi}_1$, Ψ_3, B_o, and E_c with position ζ in the macropellet are illustrated in Figure 8. These curves indicate a considerable change from center to surface of the pellet. This results from the temperature and conversion variations through the pellet.

Beck (2) has linearized the temperature dependence of the reaction rate to the form

$$\text{Rate} = a_1 + a_2 C + a_3 T \qquad (61)$$

He has shown that this approach overcompensates for temperature effects. However it does correctly indicate that effectiveness factors greater than unity are entirely feasible.

The results presented here for pelletted catalysts serve to indicate the method of solution. The same procedure could be used to obtain E_s over a range of values of $\bar{\Psi}_{1s}$, Ψ_{3s}, B_o, f, and for any micropore-size distribution. The solution of the differential equations were obtained by numerical means. Hence the same procedure could be used to compute conversion and temperature profiles, and effectiveness factors, for gel or pellet type of catalysts, and for any reaction whose rate is known.

ACKNOWLEDGMENT

This project was carried out with the assistance of Cabell Fellowship. The aid of the Northwestern University Computing Center is acknowledged.

NOTATION

A = normalization constant for pore size distribution function [Equations (29) and (30)]
A_n = frequency factor in Arrhenius rate equation
a = ratio of most probable to average pore radius
a_j = constants in Equations (29) and (30)
B_o = $E/R_g T_o$
C = concentration
D = diffusion coefficient
D' = effective diffusion coefficient in the macropores, based upon the total area (bulk diffusion)
D_e = effective Knudsen diffusion coefficient
D_B = bulk diffusion coefficient
D_k = Knudsen diffusion coefficient
E_c = effectiveness factor for a microporous particle, defined by Equation (28); $E_c{}'$ is the Thiele number, the value of E_c for the linear case with one pore size, defined by Equation (34); E_{cs} = E_c evaluated at conditions existing at the surface of a pellet.
E_s = effectiveness factor for a pellet formed by compressing microporous particles; the macroeffectiveness factor
f = fractional increase in number of moles in a reaction [Equation (46)]
$G - \beta$ = Gaussian distribution function (β = 2, 5, or infinity)
h = Thiele modulus defined by Equation (4)
k_n = surface reaction rate constant for reaction of order n; k = first-order constant
k_s = thermal conductivity of solid catalyst in microporous particle, based upon total void and solid area
k_s' = thermal conductivity of solid catalyst in a pellet, based upon total area
L = pore length
M' = molecular weight
M = Maxwellian distribution
n = order of reaction
Q = energy evolved in a reaction (Q is positive for an exothermic reaction)
R = radius of pellet
R_g = gas constant
r = pore radius
$\bar{r}$ = average pore radius, $2V_g/S_g$
r_e = effective pore radius for diffusion
$\underline{r}$ = radius vector
S_g = internal surface area per unit mass of catalyst
T = absolute temperature
V = volume
V_g = void volume per unit mass of catalyst
V_s = volume of pellet
X = conversion in the micropore = $(C_o - C)/C_o$
X_s = conversion in the pellet = $(C_s - C)/C_s$
$Z(r)$ = pore size distribution function in terms of r
$Z(\Psi_1)$ = pore size distribution function in terms of Ψ_1
z = distance from mouth of micropore ($z = 0$ at pore mouth, $z = L$ at end of pore)

Greek Letters

α = r_e/r
β = width parameter for Gaussian distribution
δ = Dirac-delta function
ϵ = void fraction
ζ = dimensionless distance in pellet, r/R
θ = dimensionless temperature in the micropore, $(T - T_o)/T_o$

θ_s = dimensionless temperature in the pellet, $(T - T_s)/T_s$
λ_g = geometry factor [Equation (51)]
λ_s = geometry factor [Equation (47)]
ξ = dimensionless distance in the micropore, z/L; $\xi = 0$ at pore mouth, $\xi = 1$ at end of pore
ρ = apparent or bulk density of the catalyst material
φ_1 = macro mass transfer parameter, defined by Equation (42)
φ_2 = macro heat transfer parameter, defined by Equation (43)
Ψ_1 = micro mass transfer parameter, defined by Equation (13)
$\bar{\Psi}_1$ = Thiele number, value of Ψ_1 when $r = \bar{r}$
Ψ_2 = micro heat transfer parameter, defined by Equation (14)
Ψ_3 = $\Psi_2/\Psi_1^{1/2}$
Λ = $(\varphi_1 E_c)^{1/2}$, defined by Equation (57)

Subscripts

e = effective
K = Knudsen
l = linear case
n = order of reaction
o = conditions at the mouth of the micropore, that is conditions at the surface of the microporous particle
s = conditions at the surface of the macropellet

Superscripts

G = Gaussian
l = linear case
M = Maxwellian
T = Thiele

Calculus

Prime = differentiation
(j) = evaluation at value of independent variable = j

LITERATURE CITED

1. Aris, Rutherford, *Chem. Eng. Sci.*, 6, 265 (1957).
2. Beek, John, *A.I.Ch.E. Journal*, to be published.
3. Bokhoven, C., and W. van Raayen, *J. Phys. Chem.*, 58, 471 (1954).
4. Harriott, Peter, Private communication.
5. Henry, John P., M.S. thesis, Northwestern University, Evanston, Illinois (1959).
6. Johnson, Marvin F. L., Private communication.
7. Kantornovick, L. V., and V. I. Krylov, "Approximate Methods of Higher Analysis," P. Noordhoff Ltd., Groningen, The Netherlands (1958).
8. Mingle, John O., Ph.D. thesis, Northwestern University, Evanston, Illinois (1960).
9. ———, and J. M. Smith, *Chem. Eng. Sci.*, to be published.
10. Present, R. D., "Kinetic Theory of Gases," McGraw-Hill, New York (1958).
11. Schilson, Robert E., Ph.D. thesis, University of Minnesota, Minneapolis, Minnesota (1958); *Dis. Ab.*, 19, 2560 (1959).
12. Smith J. M., "Chemical Engineering Kinetics," McGraw-Hill, New York (1956).
13. Sokolnikoff, I. S., and R. M. Redheffer, "Mathematics of Physics and Modern Engineering," McGraw-Hill, New York (1958).
14. Thiele, E. W., *Ind. Eng. Chem.*, 31, 916 (1939).
15. Wheeler, A., in "Catalysis," Vol. 2, p. 105, Reinhold, New York (1955).

Manuscript received August 4, 1960; revision received November 16, 1960; paper accepted November 17, 1960. Paper presented at A.I.Ch.E. New Orleans meeting.

Effective Thermal Conductivity in Packed Beds

C. D. GOPALARATHNAM, H. E. HOELSCHER, and G. S. LADDHA

Alagappa-Chettiar College of Technology, University of Madras, India

Values of the effective thermal conductivity Ke for liquids in packed beds have been obtained from heat transfer studies in such beds. The method applied by Yagi and Kunii for gases is clarified, their model is extended and is then applied to liquids. Experimental data for three different packings, glass, steel, and aluminum, with spheres of D_P/D_T ratio from 0.07 to 0.33 have been correlated. A brief comparison of the results from this analysis with previously published results from similar studies is presented.

The process of heat transfer into and through packed beds and tubes has been the subject of numerous experimental studies. Heat transfer studies in packed beds have resulted in publication of many different correlations for the effective thermal conductivity in terms of the physical and operational parameters of the systems (*1, 2, 5, 8, 15, 17, 18*). Such correlations are useful for design purposes where the conditions of the given problem are within the stated limitations of the correlation but do not generally contribute to our understanding of the physics of this process. Recently Yagi and Kunii (*14*) proposed a model for heat transfer to gases in packed beds and derived an equation which contributes considerably to an understanding of the physical processes which are of importance in determining the effective conductivity. This model is used as a starting point in the present paper. This paper presents, first, some experimental values of effective conductivity obtained for an extended range of particle to tube diameter ratios and for various liquids flowing through beds of spheres composed of either glass, steel, or aluminum. In addition a further clarification and extension of the Yagi-Kunii physical model is shown.

In the past two different types of studies in this field have been made. In the first of these effective conductivities were measured from mixed mean average temperatures inlet and outlet, known constant wall temperatures or a known constant wall heat flux rate, and the operating character-

H. E. Hoelscher is at The Johns Hopkins University, Baltimore, Maryland.